



Application of an online ion-chromatography-based instrument for gradient flux measurements of speciated nitrogen and sulfur

Ian C. Rumsey¹ and John T. Walker²

¹Department of Physics and Astronomy, College of Charleston, Charleston, South Carolina, SC 29401, USA

²Office of Research and Development, US Environmental Protection Agency, Research Triangle Park, North Carolina, NC 27711, USA

Correspondence to: Ian C. Rumsey (rumseyic@cofc.edu)

Received: 7 January 2016 – Published in Atmos. Meas. Tech. Discuss.: 22 January 2016

Revised: 10 May 2016 – Accepted: 12 May 2016 – Published: 17 June 2016

Abstract. The dry component of total nitrogen and sulfur atmospheric deposition remains uncertain. The lack of measurements of sufficient chemical speciation and temporal extent make it difficult to develop accurate mass budgets and sufficient process level detail is not available to improve current air–surface exchange models. Over the past decade, significant advances have been made in the development of continuous air sampling measurement techniques, resulting with instruments of sufficient sensitivity and temporal resolution to directly quantify air–surface exchange of nitrogen and sulfur compounds. However, their applicability is generally restricted to only one or a few of the compounds within the deposition budget. Here, the performance of the Monitor for AeRosols and Gases in ambient air (MARGA 2S), a commercially available online ion-chromatography-based analyzer is characterized for the first time as applied for air–surface exchange measurements of HNO₃, NH₃, NH₄⁺, NO₃⁻, SO₂ and SO₄²⁻. Analytical accuracy and precision are assessed under field conditions. Chemical concentrations gradient precision are determined at the same sampling site. Flux uncertainty measured by the aerodynamic gradient method is determined for a representative 3-week period in fall 2012 over a grass field. Analytical precision and chemical concentration gradient precision were found to compare favorably in comparison to previous studies. During the 3-week period, percentages of hourly chemical concentration gradients greater than the corresponding chemical concentration gradient detection limit were 86, 42, 82, 73, 74 and 69 % for NH₃, NH₄⁺, HNO₃, NO₃⁻, SO₂ and SO₄²⁻, respectively. As expected, percentages were lowest for aerosol species, owing to their relatively low deposition velocities

and correspondingly smaller gradients relative to gas phase species. Relative hourly median flux uncertainties were 31, 121, 42, 43, 67 and 56 % for NH₃, NH₄⁺, HNO₃, NO₃⁻, SO₂ and SO₄²⁻, respectively. Flux uncertainty is dominated by uncertainty in the chemical concentrations gradients during the day but uncertainty in the chemical concentration gradients and transfer velocity are of the same order at night. Results show the instrument is sufficiently precise for flux gradient applications.

1 Introduction

Development of risk assessments and mitigation strategies such as critical load frameworks (Burns et al., 2008) to protect ecosystems from nutrient and acidic deposition requires accurate speciated deposition budgets of nitrogen (N) and sulfur (S) compounds. In the United States, wet deposition has been well characterized by the National Atmospheric Deposition Program (NADP). The US Environmental Protection Agency's (US EPA's) Clean Air Status and Trends Network (CASTNet) was established in 1991 to characterize temporal and spatial trends in atmospheric concentrations and dry deposition of select N and S compounds in rural locations. Air concentrations of sulfur dioxide (SO₂), nitric acid (HNO₃) ammonium aerosol (NH₄⁺), nitrate aerosol (NO₃⁻) and sulfate aerosol (SO₄²⁻) are measured on a weekly timescale using a filter pack (Sickles et al., 1999), from which dry deposition fluxes are estimated using a multi-layer resistance model. While NADP and CASTNet are, in combination, very useful for estimating deposition of

some compounds, the N budget derived from these measurements is incomplete, particularly the dry deposition fraction. For example, fluxes of ammonia (NH_3) are not quantified. Furthermore, CASTNet dry deposition is not directly measured, but rather it is estimated using a resistance model. This model, and others used within regional chemical transport models such as the Community Multi-scale Air Quality Model (CMAQ), have not been rigorously evaluated across the range of chemical, meteorological and canopy characteristics of ecosystems for which deposition budgets are urgently needed. Thus, the dry component of total N and S deposition remains uncertain due to a lack of measurements of sufficient chemical speciation and temporal extent to develop complete annual mass budgets or of sufficient process level detail to improve current air–surface exchange models.

Over the past decade, significant advances have been made in the development of continuous air sampling measurement techniques with sufficient sensitivity and temporal resolution to directly quantify air–surface exchange of N and S compounds. With respect to N, these include bulk measurements of groups of compounds, such as fast chemiluminescence with thermal conversion for total reactive nitrogen ($\sum \text{N}_r$) (Marx et al., 2012), thermal dissociation–laser-induced fluorescence (TD-LIF) for total peroxy nitrates ($\sum \text{PNs}$) and total alkyl and multifunctional alkyl nitrates ($\sum \text{ANs}$) (Farmer et al., 2006). More selective methods for specific compounds have also emerged, including chemical ionization mass spectrometry (Sintermann et al., 2011) and tunable diode laser spectroscopy (Whitehead et al., 2008) for NH_3 , thermal dissociation–chemical ionization mass spectrometry for peroxyacetyl nitrate, peroxypropionyl nitrate and peroxyethacryloyl nitrate (Wolfe et al., 2009), and aerosol mass spectrometry for inorganic particles (Farmer et al., 2011; Nemitz et al., 2008). These methods are sufficiently fast such that fluxes may be quantified by the eddy covariance (EC) technique. However, their applicability is generally restricted to only one or a few of the compounds within the deposition budget.

NH_3 and HNO_3 , which are thought to together dominate the N deposition budget in many areas (Dennis et al., 2013), are difficult to measure due to their tendency to stick to surfaces within the sampling and analytical components of online measurement systems. For this reason, wet chemical techniques such as the Gradient of Aerosols and Gases Online Register (GRAEGOR) (Thomas et al., 2009; Wolff et al., 2010), Ammonia Measurement by ANnular Denuder sampling with online Analysis (AMANDA) (Wyers et al., 1993) and GRAdient Ammonia High Accuracy Monitor (GRAHAM) (Kruit et al., 2007) systems are the preferred methods for air–surface exchange applications. These systems are configured such that the air sample travels only a short distance (~ 0.1 m) before diffusion into solution within a wet rotating denuder. Opportunity for loss to surfaces within the sampling system are therefore minimized. A secondary benefit of the wet chemical techniques is that the use of

ion-chromatography or flow injection analysis allows for simultaneous measurement of multiple compounds, thereby minimizing the bias introduced by constructing deposition budgets from multiple measurement systems. For the NH_3 – HNO_3 – NH_4NO_3 system, simultaneous measurement of gas and aerosol components is essential to assess potential errors in fluxes related to aerosol thermodynamic instability (Wolff et al., 2010; Nemitz et al., 2004). Furthermore, simultaneous measurement of S and N compounds allows for examination of co-deposition effects between SO_2 and NH_3 related to surface acidity (Erisman and Wyers, 1993) as well as the degree of ammonium sulfate aerosol neutralization. While wet chemical techniques meet the rigorous precision and accuracy requirements of air–surface exchange applications, their temporal resolution is on the order of 30 min to 1 h. In contrast to the direct EC technique, in which air concentrations are measured at 10 Hz or faster using a single concentration measurement, fluxes must be quantified using the aerodynamic gradient method (AGM), which uses gradient concentrations at a 30 to 60 min temporal average. Furthermore using gradient concentration measurements requires additional experiments to determine the precision associated with using two sampling collection devices.

The Monitor for AeRosols and GAses in ambient air (MARGA, Metrohm-Applikon, the Netherlands) is a commercially available online ion-chromatography-based analyzer that semi-continuously measures gases and soluble ions in aerosols (ten Brink et al., 2007; Makkonen et al., 2012; Rumsey et al., 2014). The MARGA is quasi-similar to the GRAEGOR system described by Thomas et al. (2009) and Wolff et al. (2010), which has been used for flux measurements. The major difference between the MARGA 2S and GRAEGOR systems is that the MARGA employs ion chromatography for analysis of both anions and cations whereas the GRAEGOR employs ion chromatography for anions and flow injection analysis for cations. The MARGA also employs mass flow control to regulate air sampling flow rates as opposed to control by critical orifice, as in the GRAEGOR. Another difference between the GRAEGOR and the MARGA that may influence the performance of the instruments is the integration of instrument control and chromatography in the MARGA software, which includes real-time instrument performance and data quality indicators for air and liquid flows, sample collection device conditions and chromatography. The performance of the GRAEGOR in measuring air–surface fluxes has been described by Thomas et al. (2009) and Wolff et al. (2010); however, there has been no evaluation of the performance of the MARGA in measuring air–surface fluxes. Furthermore, neither the Thomas et al. (2009) nor Wolff et al. (2010) studies assessed the performance of the GRAEGOR for S compounds in comparison to empirical gradient flux data.

In this study, the performance of the MARGA in measuring gradient flux of speciated N and S is evaluated and described for the first time. This study uses a MARGA 2S

system, which is different from the MARGA 1S system described by Rumsey et al. (2014) in two key ways. First, the 2S system employs two sampling boxes interfaced to a single analytical system. The two sampling boxes in this case are positioned at two heights above the terrestrial surface to simultaneously measure the vertical concentration gradient. Second, the MARGA 2S, as configured for this work, draws the air sample through a much shorter length of tubing (30 cm) relative to the 1S configuration described by Rumsey et al. (2014).

The objective of this paper is to comprehensively evaluate and describe the performance of the MARGA in the measurement for air–surface exchange measurements of HNO_3 , NH_3 , NH_4^+ , NO_3^- , SO_2 and SO_4^{2-} . This requires two sets of experiments: one set to describe the performance of the MARGA as an analytical instrument and another to determine the performance of the MARGA as a gradient flux system. The analytical performance of the instrument is assessed by determining the accuracy, precision and analytical detection limit of the instrument using liquid standards in field conditions. To assess the performance of the MARGA as a gradient flux system, the precision of the concentration gradient which can also be defined as the gradient detection limit is determined in field conditions. The concentration gradient precision (uncertainty) and overall flux uncertainty (concentration gradient uncertainty + transfer velocity uncertainty) are then examined for a representative 3-week period over an unfertilized grass surface during the fall of 2012. A companion paper focusing on the air–surface exchange processes of individual compounds over a longer period of study is forthcoming.

2 Methods

2.1 Study site

Measurements were conducted in an unfertilized 15 ha grass field in the Blackwood Division of Duke Forest, Orange County, North Carolina, USA (35.58° N, 79.05° W). Vegetation is primarily tall fescue (*Festuca arundinacea* Shreb.), with less common species consisting of a mixture of C3 and C4 grasses, herbs and forbs (Fluxnet, 2014). The field is generally cut twice per year, once in summer and fall, and the clippings are removed for use as animal feed at local farms.

2.2 Description of MARGA gradient system

As previously mentioned, the MARGA is a commercially available online ion-chromatography-based analyzer that semi-continuously measures gases and soluble ions in aerosols. The 2S version used in this study employs two sampling boxes interfaced to a single analytical system. The two sampling boxes (SB1 and SB2) are positioned at two heights above the surface to measure simultaneous concentration gradients from which the vertical chemical fluxes are

calculated. Air is sampled through a short length (30 cm, 0.5" outer diameter) of PFA Teflon tubing with a coarse Teflon screen over the inlet to exclude large material such as insects and entrained vegetation.

Each sample box contains a wet rotating denuder (WRD) and steam jet aerosol collector (SJAC). The sample air first flows (as laminar flow) into the WRD (Wyers et al., 1993; Keuken et al., 1998), which rotates continuously so that the walls of the denuder are coated with absorption solution (double de-ionized water with 10 ppm hydrogen peroxide), ensuring that the gases diffuse into the liquid film. The level of the bulk liquid within the WRD is kept constant using a level sensor and pump connected to the absorbance solution. Particles pass through the WRD and are collected directly downstream in the SJAC (Khlystov et al., 1995). Within the SJAC, a supersaturated environment is created in which particles grow by deliquescence, allowing them to be collected by inertial separation. The supersaturated environment is created using a temperature-controlled steamer continuously supplied with absorbance solution. Air is drawn through the WRD and SJAC at 16.7 L min^{-1} using a vacuum pump (KNF model N840FT.18, KNF Neuberger, Inc., Trenton, NJ) and mass flow controller (Brooks Smart Mass Flow Controller, Brooks Instrument, Hatfield, PA). The liquid samples from the WRD and SJAC are collected in a syringe pump module located in the detector box. The syringe pump module consists of three sets of syringes: one set for the WRD, another for the SJAC and a third for the internal standard. The syringe pumps operate in tandem such that, while a set of samples is being collected, the set collected during the previous hour is being analyzed. Prior to analysis, each sample (volume = 25 mL) is mixed with an internal standard (LiBr) solution, which uses two smaller syringes (volume = 2.5 mL). Further information on the internal standard, the absorption solution and other chemical solutions used for MARGA ion-chromatography system is included in Sect. S2.2 in the Supplement. The samples are analyzed using cation and anion ion conductivity detectors (IC, Metrohm USA, Inc., Riverview, FL, USA). For the cation chromatography, the MARGA uses a 500 μL injection loop and a Metrosep C4 150 mm column (Metrohm USA, Inc.) in conjunction with a methanesulfonic acid eluent. For the anion chromatography, the MARGA uses a 250 μL injection loop and a Metrosep A Supp-10 75 mm column (Metrohm USA, Inc.) in conjunction with an eluent containing sodium carbonate monohydrate and sodium bicarbonate anhydrous.

Software integrated within the MARGA calculates atmospheric concentrations based on air sample flow rate, syringe speed during injection (relatively constant) and ion concentrations (corrected for internal standard) in the collected solutions. These results, as well as the anion and cation chromatograms and various hardware parameters, are recorded by the MARGA software.

2.3 Analytical experiments

2.3.1 Accuracy

To verify the analytical accuracy of the MARGA as controlled by the internal LiBr standard and to assess potential contamination in the liquid solutions and in the liquid flow path of the MARGA system, an experiment was conducted during field deployment using a liquid blank and four liquid external standards with different concentrations. Furthermore, the relationship between the expected and observed external standard concentrations as well as the blank concentrations were used to adjust the raw concentration data prior to flux calculations. Both the blanks and the external standards experiments were conducted with the air pumps disconnected and denuder inlets sealed. A blank was assessed using the absorption solution for a period over 24 h. The external standard test was conducted by replacing the absorption solution with a known liquid standard containing SO_4^{2-} , NH_4^+ , NO_3^- , Na^+ and K^+ . Although Na^+ and K^+ atmospheric concentrations are not the focus of this particular study, the analytical performance of the MARGA for these compounds is included to give additional information on the performance of the MARGA for a range of compounds. The ranges of concentrations for the external standard were chosen to represent the typical ambient concentrations observed at the study site. Additional information on the external standard liquid solutions is provided in Sect. S2.3.1 in the Supplement. The external standard experiments were conducted for a minimum of 12 h.

It is acknowledged that the liquid external standards used to determine accuracy do not take into account all uncertainties associated with the MARGA measurement system. In this study, it is assumed that the performance of the WRD and SJAC for collecting gases and aerosols is similar to that reported by Keuken et al. (1988), Wyers et al. (1993) and Khylostov et al. (1995), respectively. The inlet associated with the MARGA sampling system may also affect measurement accuracy, particularly for “sticky” gases such as NH_3 and HNO_3 . In this study, however, possible inlet effects were minimized by using a short length (30 cm) of PFA Teflon tubing. Cross-sensitivity of the WRD in measuring dinitrogen pentoxide (N_2O_5) as NO_3^- during the nighttime as reported by Phillips et al. (2013) may also affect the accuracy of NO_3^- measurements. In an analysis on the MARGA instrument, Phillips et al. (2013) determined that on average N_2O_5 contributed 17 % of measured nighttime HNO_3 at a sampling site near Frankfurt, Germany. The magnitude of N_2O_5 concentration varies for different geographic locations and is influenced by nitric oxide (NO) concentration, biogenic volatile organic compound concentrations and air temperature (Phillips et al., 2013). During the period of study presented here, the influence of the artifact on HNO_3 fluxes is likely small as a result of the majority of flux occurring during the daytime (owing to diurnal patterns in the momen-

tum flux; see Fig. S6 in the Supplement) and also due to the HNO_3 concentration, which is $<0.15 \mu\text{g m}^{-3}$ on average at night. Though the N_2O_5 artifact was not quantified in the current study, its potential importance for sites in the southeast US invites future investigation.

2.3.2 Analytical detection limit

The detection limit of an analytical instrument is defined as the lowest concentration that can be determined to be statistically different from a blank at a certain level of statistical confidence. In this study, the MARGA detection limit is calculated using a method from Currie (1999):

$$D_L = 2t_{1-\alpha, \nu}\sigma_o, \quad (1)$$

where σ_o is the standard deviation of the distribution of concentration when the concentration is just above the detection limit, ν is the degrees of freedom, α is the level of statistical significance and t is the Student's t statistic. The analytical detection limits of the MARGA were calculated using an observed liquid concentration after being adjusted for the internal standard.

The detection limit was determined by combining data from all analytical channels (in this study, there are four different channels including denuder and SJAC samples from both sample boxes) into a single data set. From this single data set, the standard deviation and number of analyses are used to determine the detection limit. However, using this approach means that the standard deviation may reflect a combination of random error plus systematic error between channels. To investigate this possibility, the detection limit methodology was conducted in conjunction with the Dunn's test (Dunn, 1964) and the Brown–Forsythe test (Brown and Forsythe, 1974) to compare differences across channels. Additional information on the detection limit methodology, which includes descriptions of the Dunn's test and Brown–Forsythe test methodologies, is provided in Sect. S2.3.2 in the Supplement.

When quantifying the detection limit using an external standard, the aim is to use a concentration that is slightly above the detection limit as variance may increase with increasing concentration. Therefore an appropriate external standard level was selected for each compound. In addition, two different solutions used to determine SO_4^{2-} and Na^+ detection limits allow an opportunity to investigate the relationship between concentration level and variance and thus its potential impact on the detection limit.

2.4 Gradient flux experiments

2.4.1 Aerodynamic gradient method

Air–surface exchange fluxes were quantified using the AGM. The AGM is based on the application of Fick's Law to turbulent diffusion, which relates the flux of heat, mass and mo-

mentum to the vertical gradient and turbulent transfer coefficient (eddy diffusivity) of the particular scalar of interest, in this case air concentration (C). Following Thomas et al. (2009), which is an adaptation from Thom (1975), the flux may be expressed as

$$F_x = -C_* u_* \quad (2)$$

where u_* is friction velocity, calculated from the momentum flux measured by EC, and C_* is the concentration scale calculated as

$$C_* = \frac{k}{\ln\left(\frac{z_2-d}{z_1-d}\right) - \psi_H\left(\frac{z_2-d}{L}\right) + \psi_H\left(\frac{z_1-d}{L}\right)} \cdot \Delta C. \quad (3)$$

Here ψ_H is the integrated stability function for sensible heat (Thom, 1975), z_1 and z_2 are the measurement heights above ground between which the concentration gradient (ΔC) is measured, L is the Monin–Obukhov length calculated from the EC-derived sensible heat flux, k is the von Karman constant ($k = 0.41$) and d is the zero plane displacement height, which is determined by canopy height using the relationship provided by Stanhill (1969). During the period for which fluxes are presented, average grass height within the field was 1.2 m and gradient sampling heights were 1.25 and 4.0 m above ground.

AGM fluxes were calculated from hourly average concentration gradients and hourly EC momentum and sensible heat fluxes measured above the canopy. EC momentum and sensible heat fluxes were measured with a sonic anemometer (R.M. Young model 81000V, Traverse City, MI) placed approximately 2.6 m above the ground. EC fluxes were calculated offline from 10 Hz data using SAS (SAS Institute, Cary, NC) software following standard approaches for EC. Hourly average concentration gradients were based on adjusted air concentration data. Air concentration measurements were adjusted using the internal LiBr standard, external liquid standard calibrations and air flow quality control (QC) checks. Air flow rates were independently measured at the denuder inlet at least weekly using a National Institute of Standards and Technology (NIST)-traceable primary standard (Bios DryCal DC-Lite flowmeter, Mesa Laboratories, Inc., Lakewood, CO). If the measured airflow rate was $>5\%$ different from the target airflow rate of 16.7 L min^{-1} , the MARGA mass flow controllers were recalibrated using the MARGA calibration feature, which consists of a three-point calibration at 0, 15 and 18 L min^{-1} . The MARGA software continuously records the air flow rate, which is used to calculate air concentrations from liquid concentrations. Air concentrations were also adjusted for the systematic difference in gas and aerosol concentration measurement between the sampling boxes, during co-located sampling in which the two sample boxes are positioned side-by-side. The systematic difference is determined by plotting the concentrations during the collocation against each other and calculating the slope and intercept by orthogonal least

squares regression (Wolff et al., 2010). Slope and intercepts significantly different from 1 and 0, respectively, indicate systematic error between the two boxes, which, if present, is subsequently removed prior to calculation of the concentration gradient.

2.4.2 Flux uncertainty and concentration gradient uncertainty

The flux uncertainty σ_F is calculated as (Wolff et al., 2010)

$$\sigma_F = F \cdot \sqrt{\left(\frac{\sigma_{v_{tr}}}{v_{tr}}\right)^2 + \left(\frac{\sigma_{\Delta C}}{\Delta C}\right)^2}, \quad (4)$$

where F is the flux, ΔC is the concentration gradient and $\sigma_{\Delta C}$ is the precision (uncertainty) of the concentration gradient and v_{tr} and $\sigma_{v_{tr}}$ are the transfer velocity and precision (uncertainty) of the transfer velocity, respectively. Equation (4) is used to assess the uncertainty in the measured fluxes and to quantify the relative contributions of uncertainty in chemical and meteorological measurements. In addition, each observation may be assigned a data quality indicator as being above or below the flux detection limit. v_{tr} is taken as

$$v_{tr} = \frac{u_* \cdot k}{\ln\left(\frac{z_2-d}{z_1-d}\right) - \psi_H\left(\frac{z_2-d}{L}\right) + \psi_H\left(\frac{z_1-d}{L}\right)}. \quad (5)$$

The transfer velocity and thus the uncertainty in the transfer velocity is a function of friction velocity (u_*), the measurement (z_1 and z_2) and displacement (d) heights and the integrated stability function at each height (ψ_H), which is a function of u_* , the sensible heat flux (H), buoyancy parameter (g/T), air density (ρ), specific heat (c_p) and von Karman's constant (k) (e.g., Arya et al., 2001). As noted by Wolff et al. (2010), there are no published estimates of the full uncertainty in v_{tr} . Here we approximate the uncertainty in the transfer velocity ($\sigma_{v_{tr}}$) by calculating v_{tr} using measurements of L and u_* from six co-located R.M. Young model 81000V sonic anemometers. The standard deviation of this population ($n = 6$) of measurements of v_{tr} represents a lower limit of its transfer velocity uncertainty ($\sigma_{v_{tr}}$), as uncertainty in d and ψ_H is not explicitly considered. In this case, the precision of v_{tr} was quantified as the standard deviation of the residuals of orthogonal least squares regression of v_{tr} from individual sonic anemometers against the mean for the corresponding hourly observation. The v_{tr} precision experiment was conducted adjacent to the MARGA measurement location and comprises 110 hourly observations.

The uncertainty of the gradient concentration is also quantified during co-location tests. Again, the concentrations from the two sample boxes are regressed against each using a slope and intercept from orthogonal least squares regression. The residuals of the regression represent the random error of the concentration difference between the two boxes. The standard deviation of the residuals provides a measure of the

precision of the denuder and SJAC measurements for individual analytes, which also represents the precision of the concentration gradient ($\sigma_{\Delta C}$), which can also be defined as the gradient detection limit following Wolff et al. (2010). The relationship between precision and concentration is quantified by regressing $\sigma_{\Delta C}$ on the average concentration (C) between the two boxes. Precision is expected to be a function of concentration. Therefore, concentration gradient precision was calculated at three different co-location events (June–July, August and October 2012) during the sampling periods in order to have a wide range of concentrations.

Air–surface exchange fluxes and their associated concentration gradient uncertainty and flux uncertainty were determined over 3-week representative period (23 September–14 October 2012) at the sampling site.

2.5 Ancillary measurements

A variety of meteorological parameters and surface characteristics were measured during sampling. The influence of these factors on air–surface exchange flux will be examined in the companion paper. In this paper, the meteorological parameters, wind speed, air temperature and global radiation will be presented to provide basic information on meteorological conditions during the 3-week representative period. Wind speed and air temperature were measured using the sonic anemometer (R.M. Young model 81000V, Traverse City, MI) at a height of 2.6 m. Global radiation was measured using the REBS Q7.1 net radiometer (Campbell Scientific, Logan, UT). Other surface characteristics reported in this paper include canopy height, which was measured manually and leaf area index (LAI). Single-sided LAI was measured by destructive (prior to canopy closure) and optical methods (LICOR model LAI-2000, LICOR Biosciences, Lincoln, NE)

3 Results and discussion

3.1 Analytical experiments

3.1.1 Accuracy

In the following analysis, results from liquid standard tests are expressed as equivalent air concentration unless otherwise noted. Also, though liquid standards obviously only contain dissolved ionic forms (i.e., NO_3^- , NH_4^+ , SO_4^{2-}), results are reported for both SJAC and denuder samples, adjusting for molecular weight to express denuder results in equivalent gas phase concentration (i.e., HNO_3 , NH_3 , SO_2). The results of the liquid blank are provided in Table S1 in the Supplement. Only SO_4^{2-} had a significant blank (value $> 0.001 \mu\text{g m}^{-3}$). Further analysis by an independent IC system has confirmed that both the absorption solution and the MARGA system components contribute to the SO_4^{2-} blank. The relationship between the expected and observed (re-

sponse) concentrations of the external liquid standards was investigated by regression analysis (see Fig. S1 in the Supplement). For NH_4^+ , NH_3 and K^+ there is good agreement between expected and observed concentrations, with the linear regression slopes for all compounds between 1.00 and 1.04 and offsets close to 0 (< 0.006). For Na^+ , the external standard response was not as accurate, producing slope values of 0.90 for both SB1 and SB2 and offsets of 0.013 and 0.011 for SB1 and SB2, respectively. This appears to be related to peak integration characteristics but is currently under investigation.

For the sulfur compounds (SO_4^{2-} and SO_2) associated with anion IC detection, excellent regression slopes were also observed (1.00); however, offsets (intercepts) can be observed using linear regression, which are not reflected in the blank. These offsets range from 0.09 to $0.13 \mu\text{g m}^{-3}$ for SO_2 and SO_4^{2-} . Linear regression analysis of NO_3^- and HNO_3 produced good regression slopes, ranging from 1.06 to 1.07, and similarly offsets that are not reflected in the blank, ranging from 0.05 to $0.06 \mu\text{g m}^{-3}$ (see Fig. S2). Further investigation of the difference between expected and observed concentrations for NO_3^- and HNO_3 at individual external standard levels show that the difference (observed concentration minus expected concentration) at the lowest concentration external standard (equivalent expected air concentrations are 0.131/0.126 (SB1/SB2) and 0.133/0.128 (SB1/SB2) $\mu\text{g m}^{-3}$ for NO_3^- and HNO_3 , respectively) is considerably smaller than for the other higher external standard concentrations (see Table S2 in the Supplement). Therefore, a nonlinear (quadratic) standard curve was fitted which produced slightly higher r^2 values and lower offset values in comparison to the linear fit (see Fig. S1). Thus it is hypothesized that a nonlinear response occurs at low NO_3^- concentrations. It is proposed that a similar nonlinear behavior at low concentrations may also exist for SO_4^{2-} and SO_2 . However, in this experiment, the lowest SO_4^{2-} and SO_2 external standard concentrations (expected equivalent air concentrations are 0.476/0.461 (SB1/SB2) and 0.318/0.308 (SB1/SB2) $\mu\text{g m}^{-3}$ for SO_4^{2-} and SO_2 , respectively) may have been too large to observe this nonlinearity as use of a quadratic standard curve on the SO_4^{2-} and SO_2 data did not reduce the intercept relative to linear regression. More recent results (not shown), however, support the presence of nonlinearity in SO_4^{2-} and SO_2 responses at low concentrations. These results suggest that the response is nonlinear below a SO_4^{2-} concentration of $0.27 \mu\text{g m}^{-3}$ (equivalent to a SO_2 concentration of $0.18 \mu\text{g m}^{-3}$). Therefore, it was concluded that it was more appropriate to not adjust concentrations for the linear regression slope and offset below these concentration values and to only subtract the experimentally determined blank. For HNO_3 and NO_3^- , quadratic standard curves are used for external standard adjustments and linear functions are used for the other remaining compounds.

Table 1. Detection limit (liquid and air equivalent) results incorporating data from all four channels for each analyte.

	Expected concentration ($\mu\text{g L}^{-1}$)	Median observed concentration ($\mu\text{g L}^{-1}$)	Observed standard deviation ^b ($\mu\text{g L}^{-1}$)	<i>N</i>	<i>t</i> value	Liquid detection limit ($\mu\text{g L}^{-1}$)	Air equivalent detection limit ($\mu\text{g m}^{-3}$)	
							Aerosol	Gas
NO_3^-	5.34	7.75	0.87	72	1.29	2.25	0.056	0.057
SO_4^{2-} ^a	0	1.82	0.75	142	1.29	1.93	0.048	0.032
SO_4^{2-}	19.47	26.5	1.00	72	1.29	2.58	0.064	0.043
NH_4^+	4.91	5.01	0.33	73	1.29	0.86	0.021	0.020
Na^+	1.75	1.47	0.44	73	1.29	1.15	0.029	–
Na^+	5.00	7.06	0.33	80	1.29	1.03	0.026	–
K^+	4.91	5.22	0.60	80	1.29	1.54	0.038	–

^a Detection limits for SO_4^{2-} and Na^+ were determined using two liquid standards with different concentrations.

^b ± 1 standard deviation.

3.1.2 Analytical detection limit

A summary of the detection limit analysis for each analyte is provided in Table 1. Detection limits in Table 1 were determined by incorporating data from all four channels for each analyte. Calculated detection limits were low for all compounds ranging from (in equivalent air concentration) $0.020 \mu\text{g m}^{-3}$ for NH_3 to $0.064 \mu\text{g m}^{-3}$ for SO_4^{2-} . In summary, the results of Dunn's test and Brown–Forsythe test indicate that the sampling components of the MARGA are influencing the detection limit of all the compounds except K^+ (see Sect. S3.1.2a in the Supplement). Therefore, the influence of systematic difference among channels was examined by calculating the detection limit for individual channels using Eq. (1), then averaging the four detection limits (see Table S4). Using this methodology, detection limits were lower for all the compounds that had been identified as having a significant difference in median channel concentration or channel concentration variance (all compounds except K^+) with the exception of the $1.75 \mu\text{g L}^{-1}$ Na^+ standard, which was approximately the same. The largest decrease in detection limit was for the $19.47 \mu\text{g L}^{-1}$ SO_4^{2-} standard, which decreased by $0.009 \mu\text{g m}^{-3}$. The average decrease in detection limit for the compounds was $0.004 \mu\text{g m}^{-3}$. For K^+ , the only compound that was determined to have no significant difference in median channel concentration or channel concentration variance, the detection limit was slightly higher than for the previous method ($0.038 \mu\text{g m}^{-3}$) with a value of $0.040 \mu\text{g m}^{-3}$. The NH_4^+ , NO_3^- , HNO_3 , SO_2 and SO_4^{2-} detection limits from this study (using detection limits from Table 1) are lower than those determined under field conditions in the Thomas et al. (2009) and Wolff et al. (2010) studies, which used the GRAEGOR system (see Table S5). NH_3 detection limits determined in this study are lower than those reported by Thomas et al. (2009) and Wolff et al. (2010) at a

grassland site but are similar to Wolff et al. (2010) at a forest site. This aforementioned comparison takes into account differences in the methodology used for determining detection limits. The lower detection limits observed in this study may be attributed to differences in temperature related detector stability, stability of liquid flow rates or other factors. The detection limit values as well as additional information on adjusting detection limits for different methodologies is provided in the Supplement in Sect. S3.1.2c.

3.2 Gradient flux experiments

3.2.1 Concentration gradient precision (gradient detection limit)

As previously described, the concentration gradient precision, which can also be defined as the gradient detection limit is the standard deviation of the residuals of the orthogonal least squares regression of SB1 (*y*) vs. SB2 (*x*) following Wolff et al. (2010). Scatter plots of SB1 vs. SB2 concentrations measured during three collocation experiments in June–July, August and October 2012 are included in Fig. S3 in the Supplement. The three collocation experiments consist of approximately 89, 138 and 73 hourly observations, respectively.

Results of the orthogonal least squares analysis by collocation period are summarized in Table S6 provided in the Supplement. Slopes are within ± 0.06 of unity with the exception of NO_3^- and HNO_3 during the first period, in which SB1 was lower than SB2 by $\approx 15\%$. The reason for this underestimation is not obvious. A low bias of SB1 relative to SB2 for both NH_3 and HNO_3 may indicate an effect of inlet tubing condition. Routine visual observation of the SB inlet tubing indicates that SB1, which is positioned closed to the ground, tends to accumulate dust more rapidly than SB2. As the collocation experiments are meant to serve as a QC measure for

Table 2. Summary of colocation results.

	N^a	C_{ave} ($\mu\text{g m}^{-3}$) ^b	$\sigma_{\Delta C}$ ($\mu\text{g m}^{-3}$) ^c	σ_C ($\mu\text{g m}^{-3}$) ^d	C_{max} ($\mu\text{g m}^{-3}$) ^e	C_{min} ($\mu\text{g m}^{-3}$) ^f	$\sigma_{\Delta C}/C_{ave}$ (%) ^g
NH ₃	300	0.48	0.043	0.51	3.22	0.05	9.0
NH ₄ ⁺	299	0.62	0.028	0.38	1.81	0.05	4.5
HNO ₃	282	0.61	0.035	0.60	2.52	0.03	5.8
NO ₃ ⁻	300	0.24	0.020	0.21	1.18	0.00	8.3
SO ₂	285	0.61	0.049	0.82	4.29	0.01	8.0
SO ₄ ²⁻	297	2.04	0.042	1.06	5.65	0.33	2.1

^a N is number of observations for all three colocation experiments.

^b C_{ave} is average air concentration during co-location.

^c $\sigma_{\Delta C}$ is the standard deviation of the orthogonal least squares residuals (i.e., gradient detection limit).

^d σ_C is the standard deviation of the air concentration.

^e C_{max} is the maximum air concentration.

^f C_{min} is the minimum air concentration.

^g $\sigma_{\Delta C}/C_{ave}$ (%) is the gradient detection limit expressed as a percentage of the average air concentration.

fluxes measured during the period prior to colocation, inlets are replaced after, rather than before, colocation experiments. Thus, the bias observed during colocation period 1 may reflect a dirtier inlet on SB1. This would not, however, explain the bias for NO₃⁻ aerosol unless the loss of NH₃ and HNO₃ in the inlet promoted NH₄NO₃ dissociation.

Results of the combined colocation experiments are summarized in Table 2. In general, concentrations during the three experiments were low, $<0.65 \mu\text{g m}^{-3}$, with the exception of SO₄²⁻. The gradient detection limit, defined as the standard deviation of the residuals of the orthogonal least squares regression of SB1 vs. SB2 concentrations ($\sigma_{\Delta C}$), ranges from $0.02 \mu\text{g m}^{-3}$ for NO₃⁻ to $0.049 \mu\text{g m}^{-3}$ for SO₂. The residual standard deviations determined in this study, which assume a Gaussian distribution, are considerably lower than the Gaussian standard deviations (i.e., gradient detection limits) determined by Wolff et al. (2010) for NH₃, NH₄⁺, HNO₃ and NO₃⁻, which range from $0.093 \mu\text{g m}^{-3}$ for HNO₃ at a forest site to $0.44 \mu\text{g m}^{-3}$ for NO₃⁻ at a grassland site. Expressed as a percentage of the average concentration during co-location, the gradient detection limit ($\sigma_{\Delta C}/C_{ave}$) ranges from 2.1 % for SO₄²⁻ to 9.0 % for NH₃. Unfortunately, a direct comparison of $\sigma_{\Delta C}$ expressed as a percentage of average concentration between this study and Wolff et al. (2010) study cannot be made as the average concentration during the co-location experiments is not reported by Wolff et al. (2010).

When comparing gradient detection limits, it is important to consider the relationship between concentration gradient precision and concentration. As discussed by Wolff et al. (2010), for some species the standard deviation of the orthogonal least squares residuals tends to increase with air concentration. Thus, the gradient detection limit varies with air concentration. The relationship between gradient detection limit and air concentration observed during our experiments is provided in Fig. S4. For this analysis, orthogonal least squares residuals were combined for the three coloca-

tion experiments and sorted into seven bins defined by air concentration (see Fig. S5). Within each bin, which individually contained ≈ 42 observations, the standard deviation of the residuals and corresponding bin average concentration were calculated. With the exception of NO₃⁻, all species show an increase in gradient precision with increasing concentration. In most cases, it appears that relationship between gradient precision and concentration weakens as concentrations increase. Consistent with Wolff et al. (2010), our results suggest that for some compounds, and most likely including NO₃⁻, the relationship between precision and air concentration should be considered when calculating gradient and flux detection limits at the hourly timescale. The lack of relationship observed for NO₃⁻ may be due to a relatively narrow range of low concentration observed during the colocation experiments. It is likely that this precision/concentration relationship is a general feature of the measurement system and would likely be present over a larger range of NO₃⁻ concentrations. Similar to Wolff et al. (2010), empirical functions relating gradient precision and concentration were used in this study. These were derived using the plot between bin residual standard deviation and concentration (see Fig. S4) to predict a gradient detection limit for each hourly observation based on corresponding air concentration. The relationship between gradient precision and concentration was determined using regression and are presented in Fig. S4 in the Supplement. In this study, median relative gradient detection limit uncertainty ($\sigma_{\Delta C}/\Delta C$) was 19.6 % for NH₃, 90.4 % for NH₄⁺, 29.6 % for HNO₃ and 29.2 % for NO₃⁻. These are all lower than the equivalent median relative gradient detection limit uncertainty values ($\sigma_{\Delta C}/\Delta C$) reported by Wolff et al. (2010) at a grassland site, which were 36.3, 129.6, 40.1 and 49.4 % for NH₃, NH₄⁺, HNO₃ and NO₃⁻, respectively. Thomas et al. (2009) used a different methodology to determine concentration gradient precision that is not comparable to the methodology used in this study.

3.2.2 Flux uncertainty

Of 504 possible hourly observations (during a period of 3 weeks), there were $\approx 445/380$ gradient measurements and $\approx 410/360$ flux measurements for gas/aerosol compounds, respectively. During this period, canopy height was approximately 1.2 m with a single-sided LAI of about $3.5 \text{ m}^2 \text{ m}^{-2}$. Example time series of meteorology, air concentrations and fluxes are given in Fig. S6 in the Supplement. Summary statistics for select meteorological variables, air concentrations and fluxes are provided in Table S7. Hourly air concentrations of N compounds ranged from near 0 to $\approx 2.0 \mu\text{g m}^{-3}$, with mean concentrations ranging from $0.3 \mu\text{g m}^{-3}$ for HNO_3 to $0.7 \mu\text{g m}^{-3}$ for NH_4^+ . While HNO_3 , NH_3 and NO_3^- showed distinct diurnal patterns with mid-day peaks, NH_4^+ did not. Relative to N compounds, SO_2 and SO_4^{2-} exhibited a wider range of hourly concentrations from near 0 up to 8.8 and $4.3 \mu\text{g m}^{-3}$, respectively. SO_2 displayed a distinct recurring diurnal pattern of peak concentration during the day while SO_4^{2-} temporally correlated with NH_4^+ . Average concentrations of SO_2 and SO_4^{2-} were 0.5 and $1.9 \mu\text{g m}^{-3}$, respectively.

Over the period of fluxes analyzed, air temperatures generally ranged from 5 to 10°C at night to a maximum near 25°C during the day. Wind speed and u_* ranged from near 0 at night to daytime maxima of ≈ 1.5 to 2.0 and 0.25 to 0.3 m s^{-1} , respectively. Fluxes of all compounds followed the diurnal profile of friction velocity, with peak fluxes during the daytime and fluxes near 0 at night. With the exception of NH_3 , all fluxes on average were directed toward the grass canopy. NH_3 showed a distinct diurnal profile of emissions during the day and fluxes near 0 or slightly negative overnight. As previously mentioned, a companion paper focusing on the air–surface exchange processes of individual compounds over a longer sampling period is forthcoming.

As mentioned, the concentrations used to determine concentrations gradients and thus fluxes were adjusted for the systematic difference between concentration measurements during co-location sampling. An analysis of the influence of the co-location concentration adjustment on calculated fluxes using the 3 weeks of flux values presented in this manuscript as an example is provided in Sect. S3.2.2b in the Supplement.

Individually, percentages of hourly chemical concentration gradients larger than the corresponding gradient detection limit were 86, 42, 82, 72, 74 and 69 % for NH_3 , NH_4^+ , HNO_3 , NO_3^- , SO_2 and SO_4^{2-} , respectively. As expected, percentages were lowest for aerosol species, owing to their relatively low deposition velocities and correspondingly smaller gradients relative to gas phase species. The majority of concentration gradients exceeded the gradient detection limit.

Patterns of flux uncertainty are summarized in Figs. 1 and 2. Overall uncertainty in the transfer velocity ($\sigma_{v_{\text{tr}}}$) was estimated as 0.0041 m s^{-1} ($n = 660$), which is applied as $\sigma_{v_{\text{tr}}}/v_{\text{tr}}$ to estimate the hourly fractional or per-

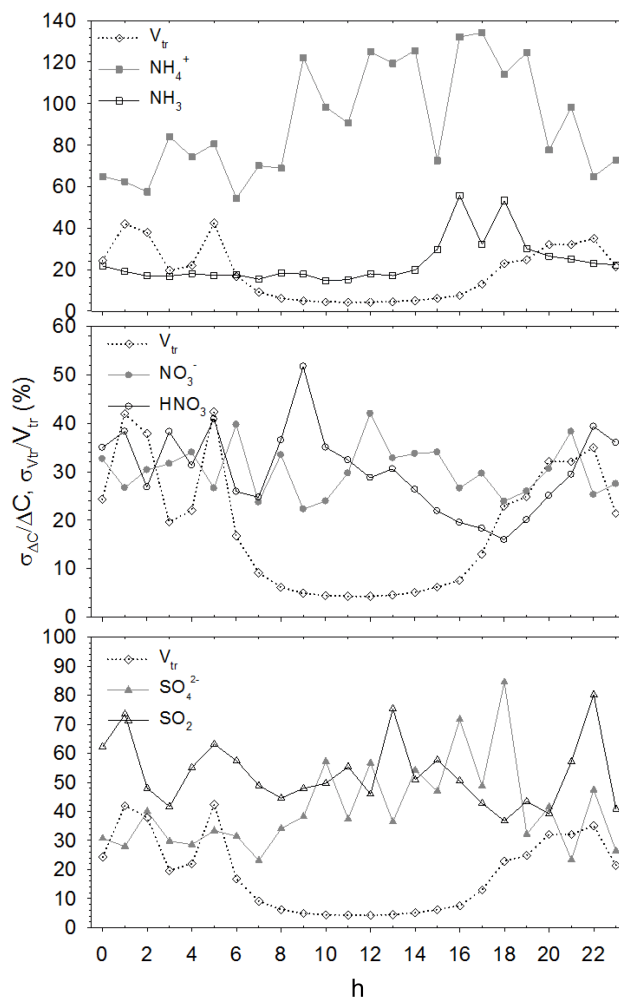


Figure 1. Diurnal profiles of uncertainty in chemical concentration gradients and transfer velocity expressed as a percentage of the corresponding concentration gradient (ΔC) and transfer velocity (v_{tr}). Data points represent median value for the corresponding hour.

centage uncertainty in v_{tr} . Figure 1 shows diurnal patterns of uncertainty in v_{tr} and chemical gradients for each compound. The graphs generally show that total flux uncertainty (Eq. 4) is dominated by uncertainty in the chemical gradients during the day but that uncertainty in the chemical gradients and v_{tr} are of the same order at night. Because the chemical gradients are influenced by air concentration and the impact of the air surface exchange process itself on the magnitude of the gradient, both of which are changing in time, diurnal patterns in uncertainty of the chemical gradient are less distinct than that of v_{tr} , which ranges from $>50\%$ at night to $\sim 5\%$ during the day. However, $\sigma_{\Delta C}/\Delta C$ generally peaks during the day when concentration gradients are smallest due to turbulent mixing. It should be noted that the largest flux uncertainty occurs at night when fluxes are near 0. Because the majority ($>90\%$) of the cumulative flux occurs

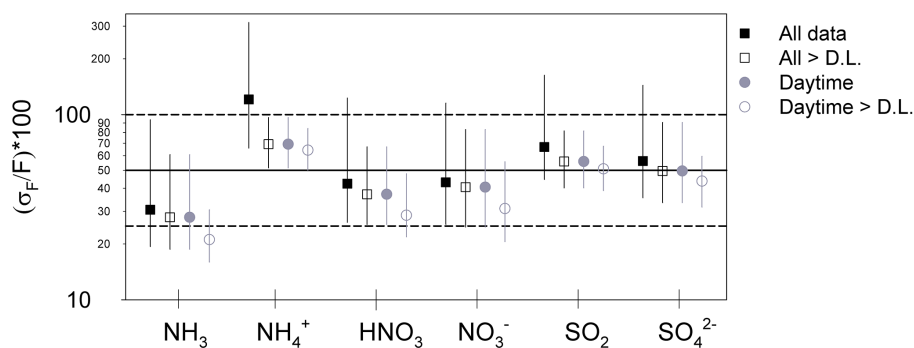


Figure 2. Summary of flux error (Eq. 4) expressed as a median percentage of the flux magnitude. Data are summarized as all data, all fluxes in which the chemical gradient exceeds the gradient detection limit, all daytime data and daytime data in which the chemical gradient exceeds the gradient detection limit. Error bars represent interquartile range.

during the day, these very large uncertainties characterize only a minor fraction of the overall flux to the ecosystem.

Total flux uncertainty is summarized in Fig. 2. When both day and night periods are considered, median total flux uncertainties are 31, 121, 42, 43, 67 and 56 % for NH₃, NH₄⁺, HNO₃, NO₃⁻, SO₂ and SO₄²⁻. Considering only concentration gradients above the gradient detection limit reduces the median uncertainties to 28, 69, 37, 41, 56 and 50 %, respectively. Flux uncertainties for N compounds are generally similar to those reported by Wolff et al. (2010). However, when comparing flux uncertainties between studies it should be acknowledged that the transfer velocity uncertainty will vary from site to site depending on meteorological conditions. Furthermore, the methodology for determining the transfer velocity uncertainty could be different, as it is between this study and the Wolff et al. (2010) study. When only daytime concentration gradients above the detection limit are considered, the uncertainties further reduce to 21, 64, 29, 31, 51 and 44 %.

4 Conclusions

This paper presents for the first time an assessment of the performance of a MARGA 2S instrument as applied for the measurement of air–surface exchange of N and S compounds. Analytical detection limits were low for all compounds ranging from 0.02 g m⁻³ for NH₃ to 0.064 g m⁻³ for SO₄²⁻. The NH₄⁺, NO₃⁻, HNO₃, SO₂ and SO₄²⁻ detection limits reported in this study are lower than those determined under field conditions in the Thomas et al. (2009) and Wolff et al. (2010) studies, both of which used the GRAEGOR system. Three collocation experiments were conducted to determine concentration gradient precision. Concentration gradient precision ranged from 0.02 µg m⁻³ for NO₃⁻ to 0.049 µg m⁻³ for SO₂. Chemical concentration gradients determined in this study compare favorably to those determined by Wolff et al. (2010). Over a period of 3 weeks in early fall 2012, we find that the majority of chemical gradients

exceed the corresponding detection limit and are therefore distinct from 0. Over the range of meteorological conditions observed, median flux uncertainty ranges from ≈ 31 % for NH₃ to ≈ 121 % for NH₄⁺. Flux uncertainties reported here for N compounds are similar to those of the GRAEGOR as reported by Wolff et al. (2010).

While the characteristics of the analytical system reported here should be generally applicable to the MARGA 2S, the assessment of gradient precision and flux uncertainty will vary to some extent for different meteorological and atmospheric chemical conditions, though not dramatically. Overall, we find that the flux uncertainties are similar to other wet chemical methods and that the instrument is sufficiently precise for flux gradient applications. It is recommended that collocation experiments be conducted regularly for long-term deployments (e.g., monthly) or for each short-term intensive deployment to properly account not only for any short-term systematic bias that may develop between the two sample boxes but also to assess the relationship between concentration gradient precision and concentration. A companion paper focusing on the air–surface exchange processes of individual compounds over a longer period of study at our site is forthcoming.

The Supplement related to this article is available online at doi:10.5194/amt-9-2581-2016-supplement.

Acknowledgements. We would like to acknowledge Rob Proost (Metrohm Applikon) and Rene Otjes (Energy Research Center, the Netherlands) for technical assistance as well as Aleksandra Djurkovic (EPA) and David Kirchgessner (EPA) for laboratory and field support. We also acknowledge Gary Lear (EPA) and Gregory Beachley (EPA) for helpful discussions regarding the MARGA instrument. This manuscript has been reviewed by EPA and approved for publication. Mention of trade names does not constitute endorsement or recommendation of a commercial product by US EPA.

Edited by: G. Phillips

References

- Arya, S. P.: Introduction to Micrometeorology, Academic Press, Cornwall, UK, 2001.
- Brown, M. B. and Forsythe, A. B.: Robust tests for equality of variances, *J. Am. Stat. Assoc.*, 69, 364–367, doi:10.1080/01621459.1974.10482955, 1974.
- Burns, D. A., Blett, T., Haeuber, R., and Pardo, L. H.: Critical loads as a policy tool for protecting ecosystems from the effects of air pollutants, *Front. Ecol. Environ.*, 6, 156–159, 2008.
- Currie, L.: Nomenclature in evaluation of analytical methods including detection and quantification capabilities (IUPAC Recommendations 1995), *Anal. Chim. Acta.*, 391, 105–126, doi:10.1016/S0003-2670(99)00104-X, 1999.
- Dennis, R. L., Schwede, D. B., Bash, J. O., Pleim, J. E., Walker, J. T., and Foley, K. M.: Sensitivity of continental United States atmospheric budgets of oxidized and reduced nitrogen to dry deposition parameterizations, *Philos. T. R. Soc. B.*, 368, 20130124, doi:10.1098/rstb.2013.0124, 2013.
- Dunn, O. J.: Multiple comparisons using rank sums, *Technometrics*, 6, 241–252, doi:10.1080/00401706.1964.10490181, 1964.
- Erisman, J. W. and Wyers, G. P.: Continuous measurements of surface exchange of SO₂ and NH₃: implications for their possible interaction in the deposition process. *Atmos. Environ.*, 27, 1937–1949, doi:10.1016/0960-1686(93)90266-2, 1993.
- Farmer, D. K., Wooldridge, P. J., and Cohen, R. C.: Application of thermal-dissociation laser induced fluorescence (TD-LIF) to measurement of HNO₃, Salkyl nitrates, Speroxy nitrates, and NO₂ fluxes using eddy covariance, *Atmos. Chem. Phys.*, 6, 3471–3486, doi:10.5194/acp-6-3471-2006, 2006.
- Farmer, D. K., Kimmel, J. R., Phillips, G., Docherty, K. S., Worsnop, D. R., Sueper, D., Nemitz, E., and Jimenez, J. L.: Eddy covariance measurements with high-resolution time-of-flight aerosol mass spectrometry: a new approach to chemically resolved aerosol fluxes, *Atmos. Meas. Tech.*, 4, 1275–1289, doi:10.5194/amt-4-1275-2011, 2011.
- Fluxnet: Duke Forest Open Field, available at: <http://fluxnet.ornl.gov/site/867>, last access: 11 September 2014.
- Keuken, M. P., Schoonebeek, C. A. M., van Wensveen-Louter, A., and Slanina, J.: Simultaneous sampling of NH₃, HNO₃, HCl, SO₂ and H₂O₂ in ambient air by wet annular denuder system. *Atmos. Environ.*, 22 (11), 2541–2548, doi:10.1016/0004-6981(88)90486-6, 1988.
- Khlystov, A., Wyers, G. P., and Slanina, J. The steam-jet aerosol collector. *Atmos. Environ.*, 29, 2229–2234, doi:10.1016/1352-2310(95)00180-7, 1995.
- Kruit, R. J. W., van Pul, W. A. J., Otjes, R. P., Hofschreuder, P., Jacobs, A. F. G., and Holtslag, A. A. M.: Ammonia fluxes and derived canopy compensation points over non-fertilized agricultural grassland in The Netherlands using the new gradient ammonia – high accuracy – monitor (GRAHAM), *Atmos. Environ.*, 41, 1275–1287, doi:10.1016/j.atmosenv.2006.09.039, 2007.
- Makkonen, U., Virkkula, A., Mäntykenttä, J., Hakola, H., Keronen, P., Vakkari, V., and Aalto, P. P.: Semi-continuous gas and inorganic aerosol measurements at a Finnish urban site: comparisons with filters, nitrogen in aerosol and gas phases, and aerosol acidity, *Atmos. Chem. Phys.*, 12, 5617–5631, doi:10.5194/acp-12-5617-2012, 2012.
- Marx, O., Brümmner, C., Ammann, C., Wolff, V., and Freibauer, A.: TRANC – a novel fast-response converter to measure total re-active atmospheric nitrogen, *Atmos. Meas. Tech.*, 5, 1045–1057, doi:10.5194/amt-5-1045-2012, 2012.
- Nemitz, E. and Sutton, M. A.: Gas-particle interactions above a Dutch heathland: III. Modelling the influence of the NH₃-HNO₃-NH₄NO₃ equilibrium on size-segregated particle fluxes, *Atmos. Chem. Phys.*, 4, 1025–1045, doi:10.5194/acp-4-1025-2004, 2004.
- Nemitz, E., Jimenez, J. L., Huffman, J. A., Ulbrich, I. M., Canagaratna, M. R., Worsnop, D. R., and Guenther, A. B.: An eddy covariance system for the measurement of surface/atmosphere exchange fluxes of submicron aerosol chemical species – First application above an urban area, *Aerosol Sci. Tech.*, 42, 636–657, doi:10.1080/02786820802227352, 2008.
- Phillips, G. J., Makkonen, U., Schuster, G., Sobanski, N., Hakola, H., and Crowley, J. N.: The detection of nocturnal N₂O₅ as HNO₃ by alkali- and aqueous-denuder techniques, *Atmos. Meas. Tech.*, 6, 231–237, doi:10.5194/amt-6-231-2013, 2013.
- Rumsey, I. C., Cowen, K. A., Walker, J. T., Kelly, T. J., Hanft, E. A., Mishoe, K., Rogers, C., Proost, R., Beachley, G. M., Lear, G., Frelink, T., and Otjes, R. P.: An assessment of the performance of the Monitor for AeRosols and GAses in ambient air (MARGA): a semi-continuous method for soluble compounds, *Atmos. Chem. Phys.*, 14, 5639–5658, doi:10.5194/acp-14-5639-2014, 2014.
- Sickles II, J. E., Hodson, L. L., and Vorbuerger, L. M.: Evaluation of the filter pack for long duration sampling of ambient air, *Atmos. Environ.*, 33, 2187–2202, doi:10.1016/S1352-2310(98)00425-7, 1999.
- Sintermann, J., Spirig, C., Jordan, A., Kuhn, U., Ammann, C., and Neftel, A.: Eddy covariance flux measurements of ammonia by high temperature chemical ionisation mass spectrometry, *Atmos. Meas. Tech.*, 4, 599–616, doi:10.5194/amt-4-599-2011, 2011.
- Stanhill, G.: A simple instrument for field measurement of turbulent diffusion flux. *J. Appl. Meteorol.*, 8, 509–513, doi:10.1175/1520-0450(1969)008<0509:ASIFTF>2.0.CO;2, 1969.
- ten Brink, H., Otjes, R., Jongejan, P., Slanina, S.: An instrument for semi-continuous monitoring of the size-distribution of nitrate, ammonium, sulphate and chloride in aerosol, *Atmos. Environ.*, 41, 2768–2779, doi:10.1016/j.atmosenv.2006.11.041, 2007.
- Thom, A. S.: Momentum, Mass and Heat Exchange, Academic Press, Chichester, UK, 1975.
- Thomas, R. M., Trebs, I., Otjes, R., Jongejan, P. A. C., ten Brink, H., Phillips, G., Kortner, M., Meixner, F. X., and Nemitz, E.: An automated analyzer to measure surface-atmosphere exchange fluxes of water soluble inorganic aerosol compounds and reactive trace gases, *Environ. Sci. Technol.*, 43, 1412–1418, doi:10.1021/es8019403, 2009.
- Whitehead, J. D., Twigg, M., Famulari, D., Nemitz, E., Sutton, M. A., Gallagher, M. W., and Fowler, D.: Evaluation of laser absorption spectroscopic techniques for eddy covariance flux measurements of ammonia, *Environ. Sci. Technol.*, 42, 2041–2046, doi:10.1021/es071596u, 2008.
- Wolfe, G. M., Thornton, J. A., Yatavelli, R. L. N., McKay, M., Goldstein, A. H., LaFranchi, B., Min, K.-E., and Cohen, R. C.: Eddy covariance fluxes of acyl peroxy nitrates (PAN, PPN and MPAN) above a Ponderosa pine forest, *Atmos. Chem. Phys.*, 9, 615–634, doi:10.5194/acp-9-615-2009, 2009.
- Wolff, V., Trebs, I., Ammann, C., and Meixner, F. X.: Aerodynamic gradient measurements of the NH₃-HNO₃-NH₄NO₃ triad using a wet chemical instrument: an analysis of precision re-

quirements and flux errors, *Atmos. Meas. Tech.*, 3, 187–208, doi:10.5194/amt-3-187-2010, 2010.

Wyers, G. P., Otjes, R. P., and Slanina, J.: A continuous-flow denuder for the measurement of ambient concentrations and surface-exchange fluxes of ammonia, *Atmos. Environ.*, 27, 2085–2090, doi:10.1016/0960-1686(93)90280-C, 1993.